

Measurement of the refractive-index structure constant, C_n^2 , and its profile in the ground level atmosphere by moiré technique

Saifollah Rasouli^a and Mohammad Taghi Tavassoly^b

^aInstitute for Advanced Studies in Basic Sciences, Zanjan 45195-1159, Iran;

^bPhysics Department, University of Tehran, Tehran 14399-66951, Iran

ABSTRACT

Atmospheric turbulence may have strong impact on astronomical imaging, aerial surveying, terrestrial geodesy, optical ranging, and wireless optical communication. Major effects are beam broadening, irradiance fluctuations (scintillation), and angle-of-arrival (AA) fluctuations. The interesting effects of atmospheric turbulence for optical propagation studies are the variation (gradient and fluctuations) of refractive index. The corresponding refractive-index structure constant, C_n^2 , is the parameter most commonly used to describe the strength of atmospheric turbulence. Besides, the Modulation Transfer Function of the atmosphere is measurable by C_n^2 . Good image quality requires C_n^2 being as small as possible. In this work we present an easily applicable and accurate method, based on moiré technique, for the measurement of C_n^2 and its profile in the ground level atmosphere. In this method from a low frequency sinusoidal amplitude grating, installed at certain distance from a telescope, successive images are recorded and stored in a computer. By rotating one of the image by $+\theta$, say 4° , and multiplying its transmission function by the transmission functions of the other images which have been rotated by $-\theta$, a large number of moiré patterns are produced. By finding the traces of the moiré fringes in the patterns, the fluctuations of the image grating lines are obtained. Which correspond to AA fluctuations distribution. From the AA fluctuations distribution in successive patterns, C_n^2 and its profile in vertical direction are deduced. This technique renders to measure some other atmospheric parameters which are discussed in the report.

Keywords: Refractive-index structure constant, moiré deflectometry, ground level atmospheric turbulence

1. INTRODUCTION

Study of atmospheric turbulence and its effects on astronomical imaging, aerial surveying, terrestrial geodesy, optical ranging, and wireless optical communication are interesting and important issues. Due to continuous and rapid changes of temperature and pressure near the ground surface, turbulences at ground levels are more severe and their effects are more pronounced. Therefore, a large number of reported works on turbulence deal with the effects of the ground level turbulence.

There are several methods for measuring the ground level atmospheric turbulence parameters, like refractive index profile and its fluctuations, correlations of the fluctuations in space and time, the atmospheric outer and inner scales, and the atmospheric refractive-index structure constant. These methods are mainly based on the measurement of the fluctuations in intensity and location of an image formed by the lights propagating in the turbulent atmosphere or the fluctuations in impinging points of narrow light beams traversing the ground level atmosphere.

Several turbulence characteristic parameters are determined by measuring the irradiance fluctuations of the image of a distant object formed by the light propagating in the atmosphere. The irradiance(intensity) fluctuations, called optical scintillation, is due to small temperature variations in random medium, resulting in refractive index fluctuations. Optical scintillation has been used to measure the inner and the outer scales of a turbulence,

Further author information: (Send correspondence to S. Rasouli)

S. Rasouli: E-mail: rasouli@iasbs.ac.ir, Telephone: 98 241 415 2062

M. T. Tavassoly: E-mail: tavasoli@iasbs.ac.ir, Telephone: 98 241 415 2122

Optics in Atmospheric Propagation and Adaptive Systems IX,
edited by Anton Kohnle, Karin Stein, Proc. of SPIE Vol. 6364,
63640G, (2006) · 0277-786X/06/\$15 · doi: 10.1117/12.683873

Proc. of SPIE Vol. 6364 63640G-1

l_0 and L_0 , the refractive-index spatial power spectrum, $\phi_n(k)$, the refractive-index structure constant, C_n^2 , and the atmospheric surface layer fluxes of heat, momentum and humidity.¹⁻⁴

In addition to scintillation, the atmospheric turbulence also induces fluctuations in the angle-of-arrival (AA) - phase tilt - and beam wanders on optical communication laser beams. The former is generally a higher frequency effect and causes the focal spot of a beam imaged through a receiving telescope to “dance” in the focal plane while the latter is a lower frequency refractive effect caused by atmospheric “cells” that are larger than the beam diameter. Some turbulence characteristic parameters are determined by measuring the AA fluctuations.⁵⁻⁷ Let us recall that the differential AA at a point on a turbulence perturbed wave front is defined as the angle between the normal to the front at the considered point and the unperturbed propagation direction. This angle is measured by different methods.

In the astronomical application the AA fluctuations measurement is a basic step for atmospheric turbulence study. The Differential Image Motion Monitor systems⁵ and the Generalized Seeing Monitor systems⁶ are established on the AA fluctuations measurement.

Edge image waviness effect⁷ is also based on the AA fluctuations measurement. The edge image motion is determined exclusively by AA, or wave-front tilt. Indeed, light waves emitted from different parts of an extended target propagate through different turbulent cells and deflect at different angles, which results in random variations of AA across the field of view(FOV). This phenomenon is commonly referred to as AA anisoplanatism. Random variations of AA across FOV cause different segments of the edge image to move independently, resulting in edge waviness. For this reason, the AA correlation scale, characterizes the edge waviness scale. Using the edge image waviness effect, the edge standard deviation has been measured and C_n^2 has been estimated.⁷

The wandering of a laser beam propagating through atmospheric turbulence arises from phase fluctuations, therefore, it is very sensitive to turbulence. The wandering and the correlation of the wanderings of two parallel beams after propagation through atmospheric turbulence are used for measuring turbulence characteristic parameters,⁸ such as the inner scale⁹ and the outer scale¹⁰ of a turbulence.

In this report we show that by installing a low frequency grating at a suitable distance from a telescope, and recording successive images of the grating by CCD camera connected to a PC, one can produce moiré patterns by superimposing the images which are rotated by a small angle θ on one of the image which is rotated by $-\theta$. By finding the traces of the moiré fringes in the patterns, the fluctuations of the image gratings' lines are obtained. These fluctuations are due to AA distribution. From the AA distribution in successive patterns, the refractive-index structure constant C_n^2 , its profile, the refractive index and temperature profiles, can be evaluated. The correlations of the AA components in the direction normal to the object grating ruling at any two points on one trace, or on two different traces can be calculated. From these correlations, the Fried's seeing parameter, r_0 , can be estimated.

2. REFRACTIVE INDEX STRUCTURE CONSTANT

As optical beams propagate along horizontal paths through the atmosphere near the Earth's surface, variations in the refractive index across the beam wave front cause random deflections in the propagation directions. The average of the deflections over an optical path is generally nonzero owing to transverse temperature and pressure gradients. Fluctuations also occur about this average. These fluctuations are related to small-scale variations in the refractive index. When the refractive turbulence is isotropic and smoothly varying, integral equations can be used to express the variance of beam AA at a transverse plane located at distance L from the target. These variations in the refractive index lead to fluctuations in intensity and location of an image formed by lights propagating in turbulent atmosphere or fluctuations in impinging points of narrow light beams traversing the ground level atmosphere.

The refractive index structure constant, C_n^2 , is an important quantity in the study of electromagnetic wave propagation in the atmospheric ground level. The performance of optical systems in the atmosphere is generally affected to some extent by the refractive turbulence along the propagation path. For example, the resolution of earth-based astronomical telescopes is often limited by the turbulence near the ground. The fading of a space-to-ground optical communication link, however, is determined by the turbulence in the higher atmosphere.

Therefore, knowledge of vertical profiles of C_n^2 would allow the performance of all types of atmospheric optical systems to be modeled. In addition, the presence of atmospheric turbulence signifies turbulent mixing of air masses of different temperatures and high-resolution vertical profiles of C_n^2 can provide insights into atmospheric dynamics.

The refractive index structure constant, C_n^2 , defined by the¹¹

$$\langle |n(\vec{x}) - n(\vec{x} + \vec{r})|^2 \rangle = C_n^2 r^{2/3}, \quad (1)$$

here n is the turbulent refractive index, \vec{x} and $\vec{x} + \vec{r}$ are two points in space, r is the magnitude of \vec{r} , and the $\langle \rangle$ denotes a time average. C_n^2 is required in parameterizing theoretical studies, for evaluating instrument design and performance, and for analyzing field data. For example, C_n^2 and the turbulence inner scale l_0 are the only two variables in the three-dimensional Tatarskii spectrum for refractive index fluctuations,

$$\phi_{3n}(k) = 0.033 C_n^2 k^{-11/3} \exp(k^2/k_m^2) \quad (2)$$

where k is the three dimensional turbulence wave number and $k_m = 5.92/l_0$. This spectrum is frequently used in modeling refractive index turbulence and thus for evaluating how electro optical systems interact with the turbulence. In one dimension, Equation (2) reduces in to the inertial-convective subrange to¹¹

$$\phi_{1n}(k) = 0.249 C_n^2 k_1^{-5/3} \quad (3)$$

where k is the one dimensional wave number. This spectrum has been useful in describing measured refractive-index spectra.

Because C_n^2 is fundamental to understanding electromagnetic wave propagation in the atmosphere, it would be useful to know how to estimate it from measured or modeled meteorological quantities. Electro-optical systems could then be optimized beforehand for the climate likely to be encountered during a field deployment.

The refractive-turbulence structure coefficient C_n^2 has been measured by many different techniques. Vertical profiles of C_n^2 extending into the stratosphere are important. This has sparked interest in developing a remote sensing capability. The principal approaches used to obtain vertical profiles have been techniques involving visible wavelength optics,¹² radar,¹³ and direct temperature fluctuation sensors.¹⁴ Recent developments of optical turbulence measurement techniques are discussed in Ref. 12.

Also, by smearing of a radial target image, the refractive index structure constant, C_n^2 , of air near the earth's surface is estimated.¹⁵ The radial target is comprised of alternating black and white sectors. By the diameter of the target image seamer region, C_n^2 is determined.

Now we present an easily applicable and accurate method, based on moiré technique, for the measurement of the atmospheric refractive-index structure constant, C_n^2 , and its profile in the ground level.

3. PHYSICAL CONSIDERATIONS

AA fluctuations are perceived as, e.g., image blurring and image motions. These fluctuations are related to the wave front of a propagating wave, which is a surface of constant phase. AA fluctuations occur when optical wave fronts passing through irregularities of the refractive index field become distorted. As radiation with a distorted wave front continues to propagate, its local irradiance also must vary under the focusing and spreading effects of that wave front. These degradation effects cause image blurring and image motions where image motion comes from the influences of large eddies moving across the aperture and image blur arises from the combination of small-scale effects and large-scale effects produced by eddies of different size. The AA, which is a measure for these effects is defined by the angle between the normal to the perturbed phase front and the normal to the unperturbed wave front, i.e., to the tangent of the direction of light propagation. This configuration is displayed in Fig. 1 where the wave is assumed to be propagating horizontally.

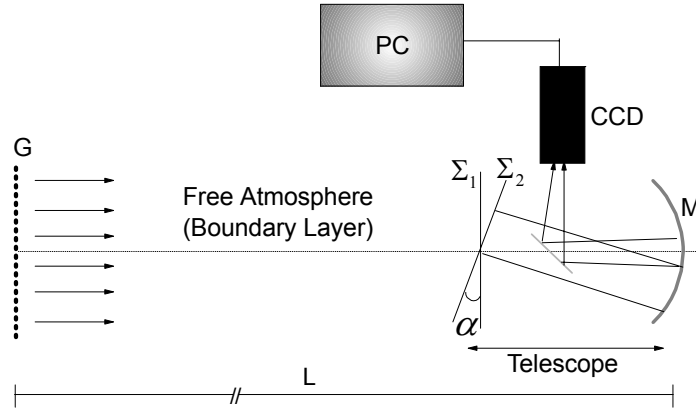


Figure 1. Schematic diagram for describing the working procedure. G , and M , stand for the sinusoidal periodic reflectance pattern, and mirror of the telescope, respectively. Σ_1 and Σ_1 , denote unperturbed and perturbed wave fronts, respectively.

Since AA fluctuations of an optical wave in the plane of the receiver aperture can be measured as slight motions of image structures, the AA fluctuation, α , can be determined using the focal length F of the imaging system. Using the geometrical relations one can find

$$\alpha = \frac{z}{F} \quad (4)$$

where z is locally displacement of image structure. Also

$$\sigma_\alpha^2 = \frac{\sigma_z^2}{F^2} \quad (5)$$

where σ_z^2 , and σ_α^2 are the variance of the motions of image structure, and the variance of the AA respectively. The determination of σ_z^2 will be discussed in the next subsection.

For a horizontal path of light, C_n^2 has the form⁷

$$C_n^2 = \frac{\sigma_\alpha^2 D^{1/3}}{1.14 L f(\frac{L_0}{D})}, \quad (6)$$

where, D is the diameter of the telescope mirror, L is the propagating length, and function $f(\frac{L_0}{D})$ describes the effect of the turbulence outer scale, L_0 , on the AA variance. This function has been quantified.¹⁶ The outer scale for propagation paths near the ground is estimated as $L_0 = 0.4h$,¹¹ where h is the altitude.

3.1. Moiré fringes displacement

Schematic diagram for describing the working procedure is shown in Fig. 1. It consists of object grating, G , imaging system, M , a CCD camera, image grabber and a PC. Σ_1 , Σ_1 , represent unperturbed and perturbed wave fronts which make angle α with each other.

Considering that z is the local displacement of a line of the image grating it can be related to the moiré fringe displacement(MFD), s , by the following formula¹⁷

$$\frac{z}{q} = \frac{s}{q_m}, \quad (7)$$

where q and q_m stand for the pitches of image grating on CCD, and the moiré pattern, respectively. Substituting from Equation (7) in Equation (4) we get

$$\alpha = \frac{z}{F} = \frac{1}{F} \frac{q}{q_m} s, \quad (8)$$

q_m and q are related by¹⁷

$$q_m = \frac{q}{2 \sin(\theta/2)} \quad (9)$$

where θ is the angle between the superimposed gratings' lines. Using Eqs (8) and (9), Equation (5) provides the variance of the AA fluctuations as

$$\sigma_\alpha^2 = \left(\frac{2 \sin(\theta/2)}{F} \right)^2 \sigma_s^2 \quad (10)$$

Finally, substituting from Equation (10) in Equation (6) we get

$$C_n^2 = \frac{4 \sin^2(\theta/2) D^{1/3}}{1.14 L F^2 f(\frac{L_0}{D})} \sigma_s^2. \quad (11)$$

3.2. Estimation of C_n^2 for slant trajectory

Measurement of the variance of the MFDs at a given point on the focal plane of telescope objective provides C_n^2 for the corresponding trajectory of the beam forming the image point. In the other word, the measurable quantity along a horizontal trajectory of the length of L at altitude z , is

$$C_n^2(z) = \frac{1}{L} \int_0^L C_n^2(x, z) dx. \quad (12)$$

For slant trajectory C_n^2 at each point depends on the altitude of the point, therefore, to obtain its mean value we should integrate along the path. Thus, for path starting at altitude z on the target grating with the optical axis of telescope at z_0 we write

$$C_n^2(z, z_0) = \frac{1}{\sqrt{L^2 + (z - z_0)^2}} \int_{(0, y, z)}^{(L, y, z_0)} C_n^2(r) dr, \quad (13)$$

Ignoring the turbulence effect in horizontal plane, we can write

$$dr = \sqrt{dx^2 + dz^2}.$$

Now according to Equation (11) and Equation (13) we can write

$$C_n^2(z, z_0) = \frac{4 \sin^2(\theta/2) D^{1/3}}{1.14 L F^2 f(\frac{L_0}{D})} \sigma_s^2(z). \quad (14)$$

If we assumed that the C_n^2 changes linearly with respect to the altitude near the ground, i.e.

$$C_n^2(z + z_0) = C_n^2\left(\frac{z + z_0}{2}\right), \quad (15)$$

and

$$C_n^2\left(\frac{z + z_0}{2}\right) = \frac{C_n^2(z) + C_n^2(z_0)}{2}, \quad (16)$$

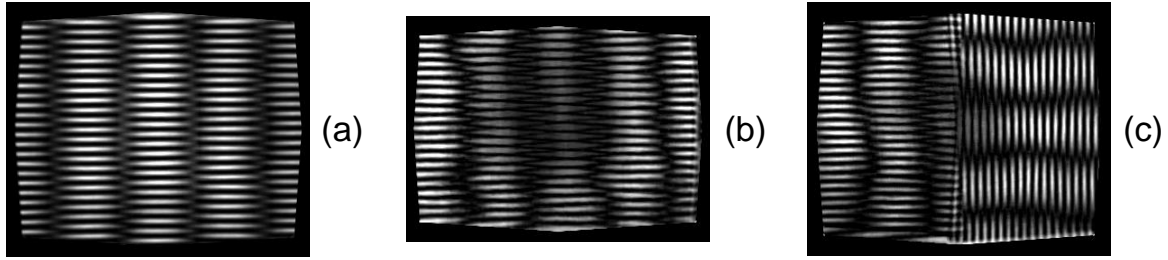


Figure 2. Two typical moiré patterns recorded at two different turbulence conditions (a), (b). The vertical and horizontal moiré patterns recorded at same time (c).

or

$$C_n^2(z) = 2C_n^2\left(\frac{z+z_0}{2}\right) - C_n^2(z_0). \quad (17)$$

For determination of $C_n^2(z_0)$, it is sufficient to take altitude of telescope in the domain of object grating height and by the Equation (14) at $z = z_0$ we have,

$$C_n^2(z = z_0, z_0) = C_n^2(z_0) = \frac{4 \sin^2(\theta/2) D^{1/3}}{1.14 L F^2 f(\frac{L_0}{D})} \sigma_s^2(z_0), \quad (18)$$

By substituting Eqs. (12) and (16) in the Equation (15), the refractive index structure constant, C_n^2 , and its profile in the ground level estimated by

$$C_n^2(z) = \frac{4 \sin^2(\theta/2) D^{1/3}}{1.14 L F^2 f(\frac{L_0}{D})} (2\sigma_s^2(z) - \sigma_s^2(z_0)). \quad (19)$$

4. EXPERIMENTAL PROCEDURE

A sinusoidal grating was programmed by a PC and printed with the period of 2.2cm on a paper of size 85cm × 66cm (being sinusoidal is not crucial). The grating was installed vertically by a wooden frame fixing its lower part 10cm above the ground. At the distance of 125m from the grating a Newtonian telescope, model 114 – 900T, was installed at a height of 70 cm over an asphalted road. The grating images were recorded by the sampling rate $25 \frac{\text{fram}}{\text{sec}}$ with a CCD camera, model *Sony, XC – 57CE*, and fed to the PC.

Several sets of data corresponding to low, medium, and high turbulence conditions were digitized with a frame grabber. In this report, we refer to two series of measurements performed on 5 and 27 October 2005, at cloud free and moderately windy conditions. Each set of data was collected in 120sec and consisted of 3000 frames. Using Matlab software the first frame was rotated by an angle equal to 4° and multiplied by the other frames rotated by –4° to produce the required moiré fringes. The sample moiré fringes are shown in Fig. 2.

The traces of moiré fringes can be specified by different methods. But, we found the following method more suitable. The intensity distribution in the neighborhoods of the moiré dark fringes is specified. The fluctuations in intensity reduce by approaching to a moiré dark fringe. The contour of the least fluctuations (the least visibility) is the trace of the moiré dark fringe. By this method the traces of the moiré fringes can be determined by one pixel accuracy. A single moiré dark fringe, the visibility distribution in its neighborhood, and the dark fringe trace, are shown in Fig. 3(a), (b), and (c), respectively.

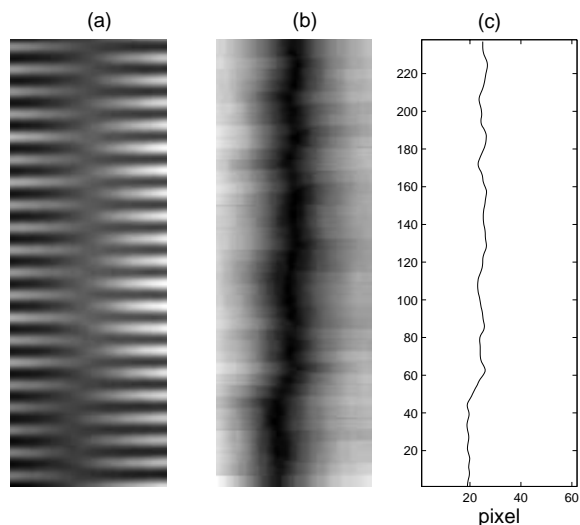


Figure 3. A sample moiré dark fringe (a), the visibility distribution in the area containing the dark fringe (b), and the trace of the dark fringe (c).

4.1. Moiré fringe displacement analysis

Once all 3000 data frames in the data set are processed, the MFD statistics, including mean fringe trace, fringe displacement standard deviation, and displacement correlation function are calculated from the corresponding time series. For a point on a moiré trace, the mean position is given by

$$\bar{e}[i] = \frac{1}{N} \sum_{j=1}^N e[i, j], \quad (20)$$

where $e[i, j]$ is the moiré fringe position for the i th row (or column) in the j th frame, $N = 3000$ is the number of frames, and the overbar denotes mean value over time. We define the MFD as, $s[i, j] = e[i, j] - \bar{e}[i]$. Thus, the MFD standard deviation can be given by

$$\sigma_s[i] = \left\{ \frac{1}{N-1} \sum_{j=1}^N (s[i, j])^2 \right\}^{1/2}. \quad (21)$$

4.2. Experimental Results

The component α of the AA fluctuations in the direction perpendicular to the lines of the object grating (parallel to the moiré trace) is given by:

$$\alpha[i, j] = \frac{2 \sin(\theta/2)}{F} s[i, j], \quad (22)$$

where, F is the focal length of the telescope mirror, and θ is the angle between the rulings of the superimposed grating images. The plot in Fig. 4 show the vertical component of AA fluctuations, at an arbitrary point versus time for one set of data.

A typical single moiré dark fringe dancing at different time in the presence of turbulence are shown in Fig. 5. All of patterns have 0.4sec respect together.

As mentioned in Equation (6), for a horizontal path of light, the C_n^2 has the form⁷

$$C_n^2[i] = \frac{\sigma_\alpha^2[i] D^{1/3}}{1.14 L f \left(\frac{L\theta}{D} \right)}, \quad (23)$$

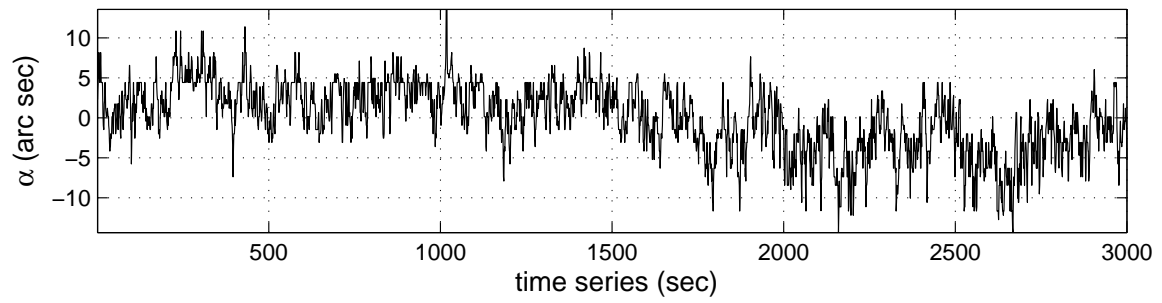


Figure 4. Typical the vertical component of AA fluctuations at a point versus time.

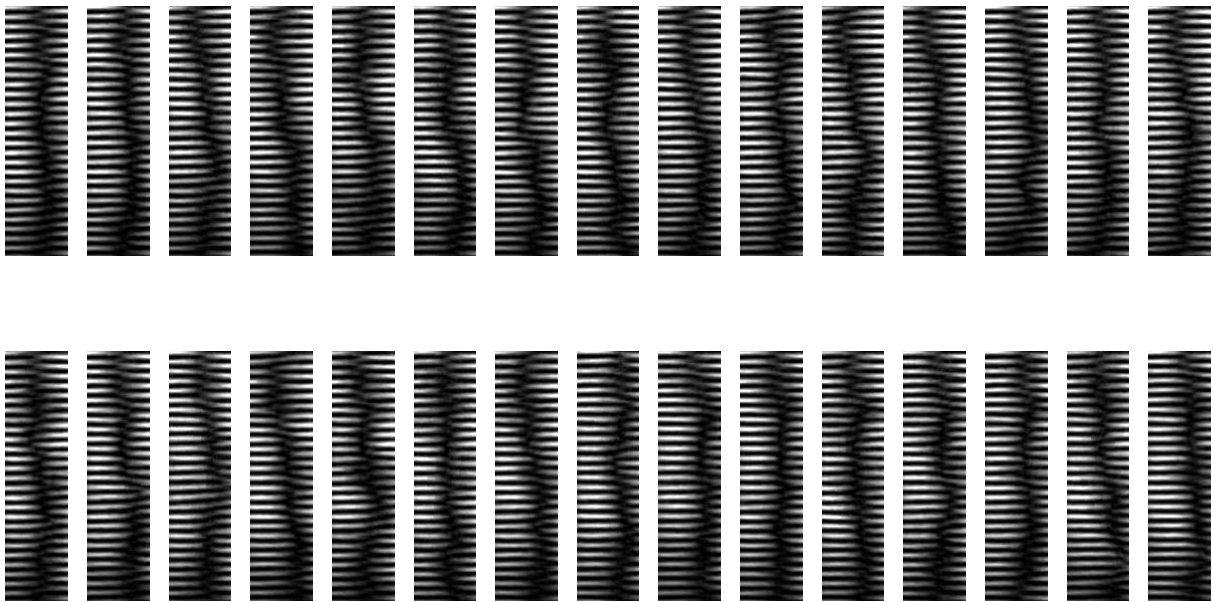


Figure 5. The successive images of a moiré dark fringe recorded at the time intervals of 0.4sec. in turbulent atmosphere.

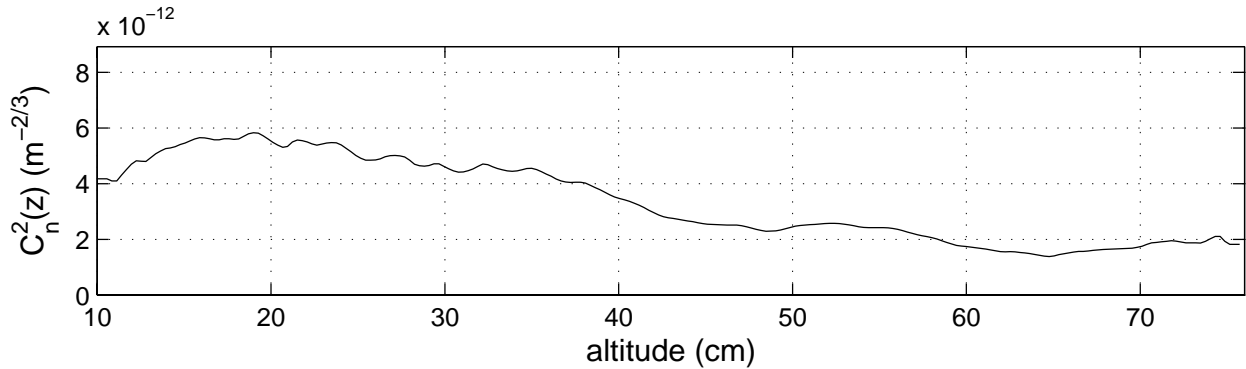


Figure 6. The refractive index structure constant profile at a vertical direction

where, $\sigma_\alpha^2[i]$ is the AA variance at i th row (or column). As mentioned function $f(\frac{L_0}{D})$ describes the effect of the turbulence outer scale, L_0 , on the AA variance. In the von Karman model, For $h = 75\text{cm}$, and $D = 114\text{mm}$, the predicted value of $f(\frac{L_0}{D})$ is 0.6.¹⁶ Using Equation (23) the refractive index structure constant profiles at vertical direction for the data set recorded at 14:17 (27 Oct. 2005) is shown in Fig 6. Unfortunately, independent measurements of C_n^2 during the test were not performed. Under these circumstances we can only compare the measured values of C_n^2 with typical values of C_n^2 obtained by other techniques.

The local MFD is a measure of AA component in the direction perpendicular to the object grating lines. Thus, by measuring the displacements of moiré traces over the entire image, we can get the distribution of the latter AA component. Also, by changing the angle between the rulings of the image gratings and shifting one of image grating with respect to the other the mentioned distribution can be obtained by desired scale. By changing the direction of the object grating by 90° the distribution of the other component is obtained. This can be done simultaneously by using an object grating with two part having perpendicular rulings, Fig. 2(c).

4.3. Atmospheric turbulence, Moiré technique and Correction methods

Often, the two-dimensional spatial covariance of AA fluctuations is used to investigate the properties of wave fronts corrugated by the atmosphere.¹⁸ The covariance of the AA fluctuations in the image plane can be defined by¹⁹

$$B_\alpha(\mu, \eta) = \frac{\langle \alpha(x, y)\alpha(x + \mu, y + \eta) \rangle}{\sigma_{\alpha(x, y)}\sigma_{\alpha(x + \mu, y + \eta)}}, \quad (24)$$

where (x, y) and $(x + \mu, y + \eta)$ are coordinates of two arbitrary points of the distance $\sqrt{\mu^2 + \eta^2}$, and $\langle \rangle$ denotes statistical averaging. This covariance can be attributed to the correlation of the turbulences in the optical paths of the lights forming the images. The plots in Fig. 7(a) and (b) are the longitudinal simultaneous covariances (in the tilt direction), B_l , corresponding to the moiré fringes in Fig. 2(c) in the object scale. The plots in Fig. 7(c), specified by (1), (2), and (3) are B_l s for three different turbulence conditions for the aperture diameter $D = 114\text{mm}$.

4.3.1. Aperture Averaging Effect

If the receiving aperture is less than some critical size, such that the AA fluctuations are correlated over its area, then the aperture will behave as a point detector. As the aperture size increases so that the AA fluctuations are uncorrelated over the aperture, then the intensity is a spatial average over some finite region of space, and the fluctuations tend to decrease. This is a well-known experimental effect in astronomical observations with a telescope. The angle of arrival corresponds to the normal to the wave front.

We feel that the moiré technique have a high potential for correction methods in the atmospheric turbulence studies. In this paper the aperture averaging effect on the AA fluctuations was study. The turbulence conditions

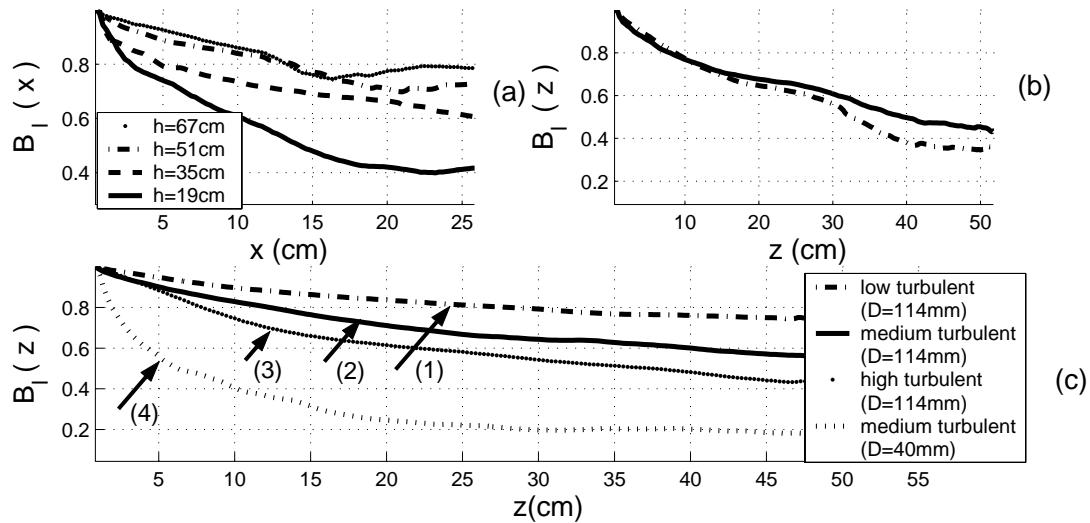


Figure 7. Simultaneous longitudinal covariances of the AA (B_l) at four different levels in horizontal direction, (a), and at two different locations in vertical direction, (b). The covariances B_l at three different turbulence conditions, (1), (2), and (3), and different aperture diameter (4), (c).

for curves (2) and (4) in the fig. 7, were the same, but they differ due to aperture averaging effect. The diameter of the aperture for the latter was $D = 40$ mm.

As the variances of longitudinal and lateral differential image motion are related to Fried's seeing parameter, r_0 ,^{5,20} by measuring the variances of differential displacements of two points on a moiré trace, or two points on two abutting moiré traces, r_0 can be evaluated.

5. CONCLUSION

We see that the moiré technique, is an effective, and reliable method for measuring turbulence parameters that are based on AA fluctuations. Since the differential displacement measurement is not affected by small motion of the object grating, it seems that by installing a suitable grating on a balloon and recording its images from a base on the ground, the atmospheric parameters in vertical direction can be evaluated which astronomers are interested in.

Besides, inclusion of moiré technique provides two dimensional map of AA fluctuations which leads to more accurate correlation calculation and profile evaluation.

In the present approach after the filed process, by superimposing the images of the grating the moiré patterns are formed. Thus observation of the AA fluctuations visually improved by the moiré magnification, but it was not increased precision of the AA fluctuations measurements. Parallel to this work we show that in a rather different experimental approach a high precision AA measurement of fluctuations based on moiré fringe displacements.²¹ In the latter method application of moiré technique improved measurement precision more than 10 times.

REFERENCES

1. L. C. Andrews, R. L. Phillips, C. Y. Hopen, and M. A. Al-Habash, "Theory of optical scintillation," *J. Opt. Soc. Am. A* **16**, pp. 1417–1429, 1999.
2. R. J. Hill, "Comparison of scintillation methods for measuring the inner scale of turbulence," *Appl. Opt.* **27**, pp. 2187–2193, 1988.
3. A. Consortini, E. Cochetti, J. H. Churnside, and R. J. Hill, "Inner-scale effect on irradiance variance measured for weak-to-strong atmospheric scintillation," *J. Opt. Soc. Am. A* **10**, pp. 2354–2362, 1993).

4. R. J. Hill, "Review of optical scintillation methods of measuring the refractive-index spectrum, inner scale and surface fluxes," *Waves in Random Media* **2**, pp. 179–201, 1992.
5. M. Sarazin and F. Roddier, "The ESO differential image motion monitor," *Astron. Astrophys.* **227**, pp. 294–300, 1990.
6. A. Ziad, R. Conan, A. Tokovinin, F. Martin, and J. Borgnino, "From the grating scale monitor to the generalized seeing monitor," *Appl. Opt.* **39**, pp. 5415–5425, 2000.
7. M. S. Belen'kii, J. M. Stewart, and P. Gillespie, "Turbulence-induced edge image waviness: theory and experiment," *Appl. Opt.* **40**, pp. 1321–1328, 2001.
8. A. Consortini, and K. A. O'Donnell, "Beam wandering of thin parallel beams through atmospheric turbulence," *Waves in Random Media* **3**, pp. S11–S28, 1991.
9. C. Innocenti, and A. Consortini, "Estimate of characteristic scales of atmospheric turbulence by thin beams: comparison between the von Karman and Hill-Andrews models," *Journal of modern optics* **51**, pp. 333–342, 2004.
10. A. Consortini, C. Innocenti, and G. Paoli, "Estimate method for outer scale of atmospheric turbulence," *Optics Communications* **214**, pp. 9–14, 2002.
11. V. I. Tatarskii, *Wave Propagation in a Turbulent Atmosphere*, McGraw-Hill, New York, 1961.
12. F. D. Eaton, "Recent developments of optical turbulence measurement techniques," in *Atmospheric Propagation II*, C. Y. Young, and G. C. Gilbreath, ed., *Proc. SPIE* **5793**, pp. 68–77, 2005.
13. R. Earl Good, B. J. Watkins, A. F. Quesada, J. H. Brown, and G. B. Loriot, "Radar and optical measurements of C_n^2 ," *Appl. Opt.*, **21**, pp. 3373–3376, 1982.
14. R. S. Lawrence, G. R. Ochs, and S. F. Clifford, "Measurements of Atmospheric Turbulence Relevant to Optical Propagation," *J. Opt. Soc. Am.*, **60**, pp. 826–830, 1970.
15. A. S. Gurvich, I. S. Starobints, and K. A. O'Donnell, "A method of determining the structure characteristic of the index of refraction in the atmosphere from the image of a radial target," *Izv. Atmospheric and Oceanic Physics*, **10**, No. 4, pp. 413–417, 1974.
16. R. J. Sasiela and J. D. Shelton, "Transverse spectral filtering and Mellin transform techniques applied to the effect of outer scale on tilt and tilt anisoplanatism," *J. Opt. Soc. Am. A*, **10**, pp. 646–660, 1993.
17. K. Patorski, *Handbook of the Moiré fringe technique*, Elsevier, Amsterdam, 1993.
18. R. Conan, J. Borgnino, A. Ziad, and F. Martin, "Analytical solution for the covariance and for the decorrelation time of the angle of arrival of a wave front corrugated by atmospheric turbulence," *J. Opt. Soc. Am. A* **17**, pp. 1807–1818, 2000.
19. F. Roddier, "The effects of atmospheric turbulence in optical astronomy," in *Progress in Optics XIX*, E. Wolf, ed., North-Holland, 1981.
20. Y. Zhang, D. Yang, and X. Cui, "Measuring seeing with a Shack-Hartmann wave-front sensor during an active-optics experiment," *Appl. Opt.* **43**, pp. 729–734, 2004.
21. S. Rasouli, and M. T. Tavassoly, "Application of moiré technique to the measurement of the atmospheric turbulence parameters related to the angle of arrival fluctuations," submitted to the *Optics. Letters*. 2006.